OPEN ACCESS
Journal of Multidisciplinary Applied Natural Science Vol. 5 No. 2 (2025) https://doi.org/10.47352/jmans.2774-3047.253
Check for updates
Research Article

Assessment of LINAC Source Radiation Dose around Healthy Organs Using Treatment Planning System Calculation

Ramacos Fardela*, Ega Septryan Candra, Dian Milvita, Dedi Mardiansyah, Ridwan Ridwan, Fiqi Diyona, and Almahdi Mousa

Received : September 3, 2024	Revised : February 2, 2025	Accepted : February 14, 2025	Online : March 3, 2025

Abstract
The negative effects of increased radiation dose can impact healthy tissue surrounding the target area, necessitating careful management to minimize side effects and meticulous planning in radiation therapy. This study aims to determine the peripheral dose of a 6 MV photon beam and compare the measured values with the estimates from the Treatment Planning System (TPS). Dose calculations were performed using the Analytical Anisotropic Algorithm (AAA) in the ECLIPSE^{TM} TPS on a virtual water phantom with a 6 MV photon beam, delivered by a Clinac CX linear accelerator (LINAC) at Unand Hospital. Photons were used with variations in target depth of 1.5, 5, and 10 cm, as well as variations in measuring distances of 3, 5, 7, 10, and 15 cm outside the irradiation field. The area of irradiation used varied of 5×5 and 10×10 cm^2. The measurement results based on the distance of the field edge showed that the dose percentage decreased below 10% when passing a distance of 5 cm for a field area of 5×5 cm^2, and for a field area of 10×10 cm^2, the dose percentage decreased below 10% after passing a distance of 7 cm from the edge of the irradiation field. The peripheral dose intensity in the area outside the target will decrease along with the increasing measurement distance from the edge of the field and the depth due to the interaction of radiation with the medium, which causes the spread and absorption of photons in the medium.

Keywords: peripheral dose, photons, LINAC, treatment planning system

1. INTRODUCTION

X-rays are electromagnetic radiation with a wavelength of 10^{-11}–10^{-8} m, a frequency of 10^{16}–10^{20} Hz, and an energy of 100 eV to 100 keV for diagnostic radiology and high energy (MeV) X-rays for radiotherapy [1]-[3]. Radiotherapy, a cornerstone of modern medicine, is an essential tool in treating various medical conditions, particularly in cancer care [4]-[6]. Radiation exposure can induce both stochastic and deterministic biological effects. Stochastic effects are probabilistic; the likelihood of an effect increases with higher doses, while the severity remains constant. In contrast, deterministic effects exhibit a clear dose-response relationship, with severity escalating as the dose increases [7][8]. Radiotherapy must be optimized at the target volume corresponding to the effective dose received without causing significant damage to the surrounding normal tissue [9]. The main goal of radiation therapy is to induce ionizing radiation with an optimal dose on the target cancer or tumor that causes damage to DNA so that it will kill the cancer cells. The effects of radiation therapy not only kill cancer cells but also affect healthy tissue around the target [10]-[12].

Radiation that hits a tissue will affect the properties of the tissue. Its effects are divided into three types, namely physical, chemical, and biological effects [13]. The first effect that will appear when this radiation exposure occurs is the physical effect. This physical effect can be in the form of excitation and ionization. Excitation is a process where particles hit electrons from the innermost shell, but it does not cause the electrons to be lost; it only moves to the outer shell because the particles lack the energy to remove the electrons [14].

This effect occurs normal cells or tissues around the cancer target are exposed to radiation. The severity of damage to healthy tissue around the cancer can be grouped into stochastic and deterministic effects. Deterministic effects depend on exposure time, dose, and type of radiation. This effect has a dose threshold. The consequences of these effects could not be directly felt by the patient. Stochastic effects occur in patients without any influence from the dose threshold. This effect depends on how much of the dose healthy tissue absorbs. To minimize the negative effects of radiation, proper planning and optimization of

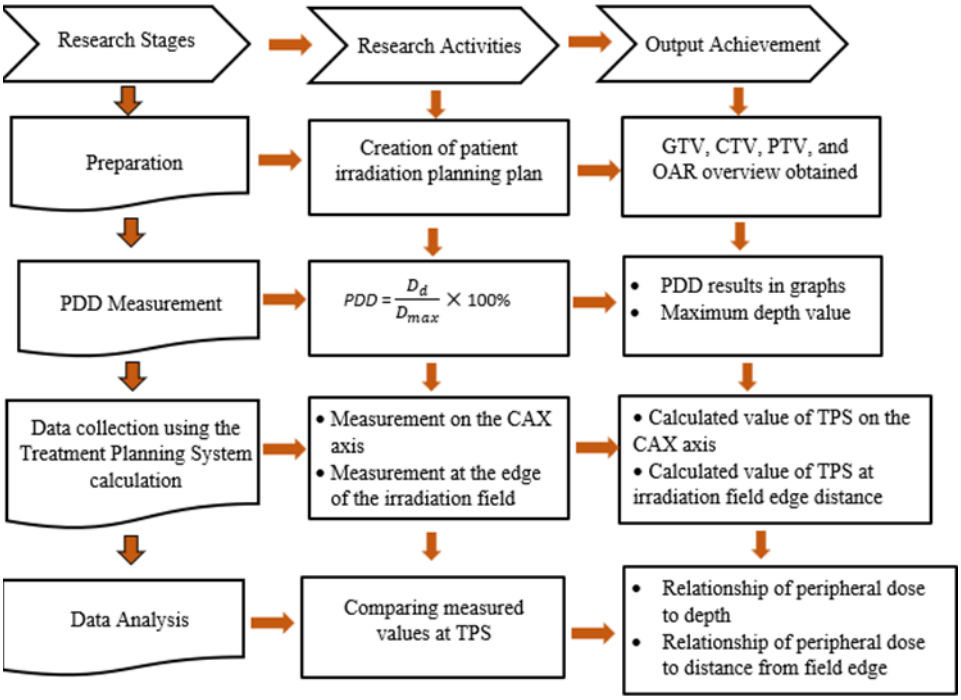

Figure 1. Research flow chart.

radiation doses are essential [15].

Dose calculations can be performed using the Treatment Planning System (TPS). TPS is a software system used in radiotherapy to plan and calculate the radiation dose needed to treat cancer in patients. TPS allows medical physicists to plan external radiation exposure or brachytherapy by considering several factors, such as cancer location, size, and tissue sensitivity around the radiation target. TPS can determine the amount and direction of radiation exposure needed to match the desired dose while minimizing the dose to healthy tissue around it. Patient data such as CT scan images create a three-dimensional model of the target area and surrounding healthy tissue, allowing for accurate radiation dose calculations ysing complex mathematical algorithms [16].

Radiation therapy using intensity-modulated radiation therapy (IMRT) or volumetric-modulated radiation therapy (VMAT) techniques requires more accurate radiation modeling so that the radiation dose for small or large irradiation fields does not have excessive scattering. The effect of lateral scattering on radiation beams and radiation inhomogeneity is one of the factors that must be considered before radiation delivery [17][18]. This factor will continue to be taken into account when planning therapy using TPS. According to Diallo et al., accurate and precise dose calculation is a critical assessment during radiotherapy treatment. Most secondary cancers have developed in the peripheral area of the target volume, ranging from 2.5 cm inside to 5.0 cm outside the irradiated area [19]. Peripheral dose is the radiation dose of healthy tissue outside the cancer target. The peripheral dose value that hits the patient's body can be caused by several factors, such as leakage in the gantry, scattered radiation in the collimator, or the presence of internal scattering from the patient or phantom (backscattered factor) [20]-[22]. The objective of this study is to determine the target volume in the TPS and to analyze the peripheral dose distribution received by healthy tissues outside the therapy target area. Lower peripheral doses can reduce toxicity, improve quality of life, and potentially increase overall survival rates in cancer patients. Reducing the peripheral dose helps protect healthy tissue adjacent to the tumor from unnecessary radiation exposure, which is especially important in sensitive areas where damage can lead to significant complications or secondary cancers [23][24].

2. MATERIALS AND METHODS

2.1. Materials

TPS was used to design radiotherapy beams on

LINAC [25][26]. Dose calculation was done on TPS from ECLIPSE™ using the Analytical Anisotropic Algorithm (AAA) on a virtual water phantom. The AAA provides a more accurate dose estimation in the region surrounding the tumor, including peripheral doses. It offers superior modeling of radiation scatter effects, which is crucial for calculating doses beyond the primary radiation field boundaries. This capability is particularly beneficial in advanced treatment techniques such as IMRT and VMAT, where complex dose distributions are required. However, AAA has certain limitations, including its dependence on accurate input data, constraints in specific clinical scenarios, sensitivity to material effects, computational complexity, and the necessity for validation and calibration [27]-[29].

2.2. Methods

2.2.1. LINAC Radiotherapy Planning

Calibration involves verifying that the TPS accurately predicts the dose distribution based on the treatment plan and beam characteristics. The TPS calibration process can be conducted by measuring beam characteristics. This calibration is performed by collecting data such as percentage depth dose (PDD), tissue maximum ratio (TMR), output factors for various field sizes, and beam profiles at different depths [30]. Radiotherapy planning for patients was done by determining the target radiation volume and the uniformity of the dose received on the cancer target [31]. Patient planning on TPS was done by creating a picture of the Gross Tumor Volume (GTV), Clinical Target Volume (CTV), Planning Target Volume (PTV), and Organ at Risk (OAR) sections. The flow chart in the study can be seen in Figure 1.

2.2.2. PDD Measurement

PDD measurements were taken to obtain the maximum depth value of the 6 MV beam. PDD can describe the dose distribution at each point in a radiation field with a certain depth. The calculation of the PDD value can be done using Equation 1. D_d is the radiation dose (cGy), and D_{max} is the maximum depth dose (cGy) [32].

$$PDD = \frac{D_d}{D_{max}} \times 100\% \quad (1)$$

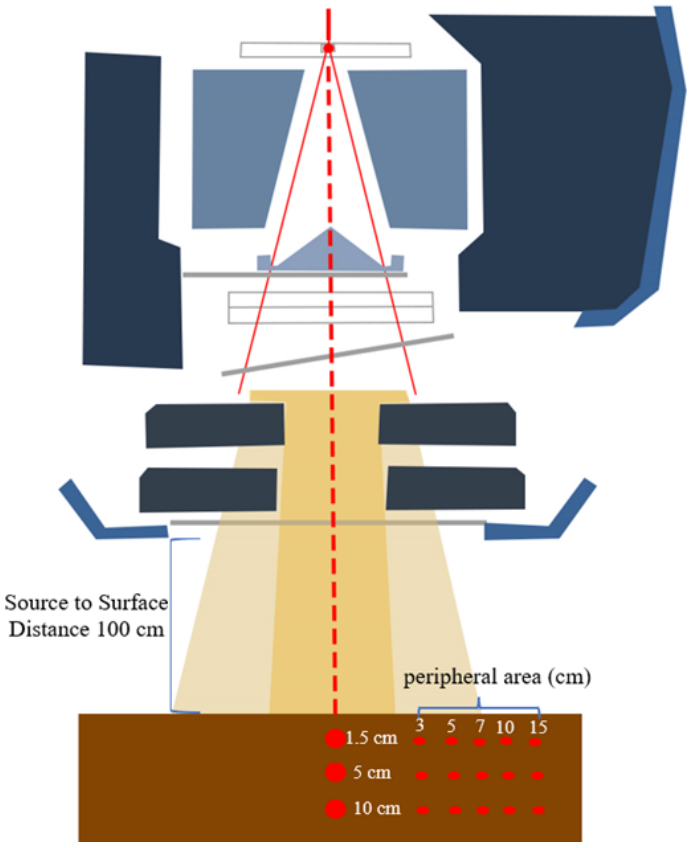

Figure 2. Treatment planning system dose calculation scheme.

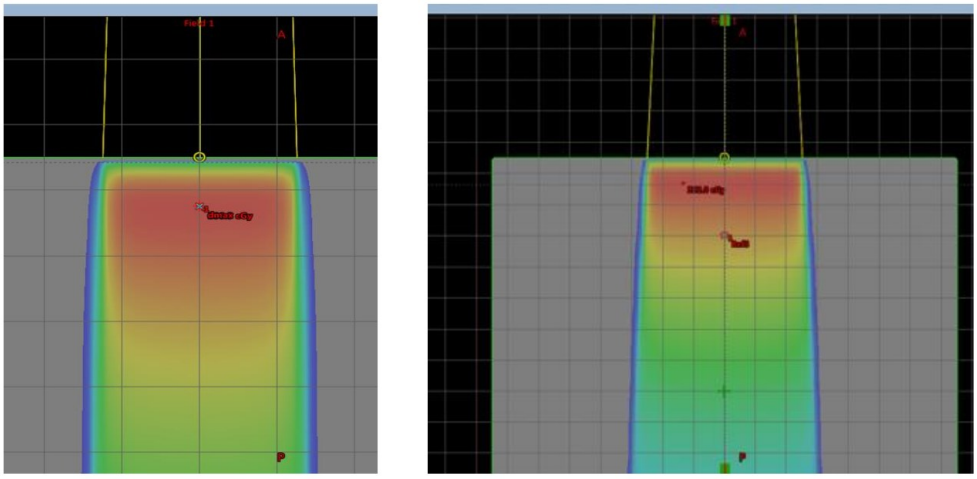

(a) (b)

Figure 3. Planning target field area of (a) 5×5 and (b) 10×10 cm^2.

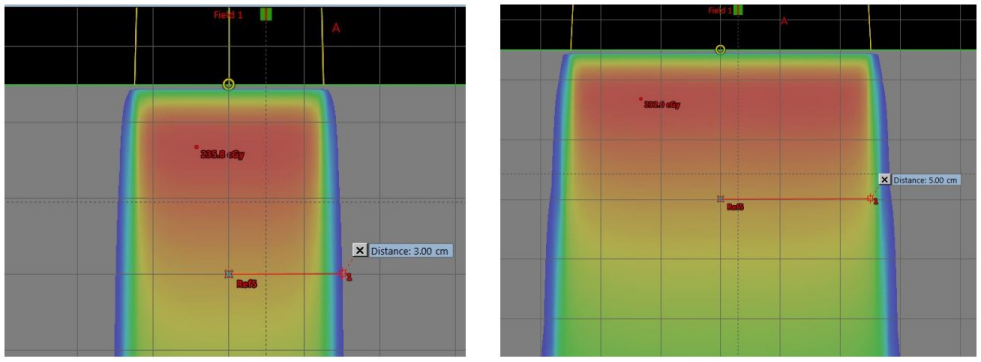

(a) (b)

Figure 4. Peripheral area of the field area of (a) 5×5 and (b) 10×10 cm^2.

2.2.3. TPS Dose Calculation

Calculation by TPS begins with planning the irradiation with the MU value used as 100 MU. Measurements are made using TPS, where TPS will design the estimated dose for the cancer target. The system has set the MU value in the TPS calculation. The calculation by TPS begins with creating an irradiation plan that will be carried out. After the planning, TPS will calculate the dose received at the measurement point. Peripheral dose calculations were performed at depths of 1.5, 5, and 10 cm with distance variations of 3, 5, 7, 10, and 15 cm from the edge of the radiation field. The field areas used were 5×5 and 10×10 cm^2. The scheme of peripheral dose calculation in TPS can be seen in Figure 2.

2.2.4. Normalization of Measurement Result

The measurement results that were read will be normalized to the main axis of the central axis (CAX) beam as the off-axis ratio using Equation 2;

$$PD = \frac{M}{M_{CAX}} x\ 100\% \quad (2)$$

where PD is the peripheral dose, M is the the value from the detector at the measurement point, and M_{CAX} is the value from the detector on the main axis of the beam [33][34]. The measurement results are analyzed by comparing the measured peripheral dose with the expected value calculated by the TPS. This comparison helps identify discrepancies and assess the accuracy of the dose distribution obtained from measurements relative to TPS calculations [35].

3. RESULTS AND DISCUSSIONS

3.1. Cancer Target Volume in TPS

Determination of target volume in TPS can be seen in Figure 3. Figure 3 shows the comparison of the doses received by the target volume. Figures 3 (a) and 3(b) are the target plan for a field area of 5×5 and 10×10 cm^2. The cancer target with the

maximum dose is marked in red, where this area is where the GTV is located. The caption D_{max} in the figure is the maximum depth. The D_{max} in the study was at a point of 1.5 cm, and the maximum dose value was 200 cGy. The orange color in TPS represents the CTV area. The yellow color represents PTV, the green color represents OAR, and the peripheral area is marked in blue. Each target area has a different dose value. The measured radiation dose value will decrease with each color change of the target area in the TPS.

The dose value is lower for areas that are further from the target. In a field area of 5×5 cm^2, the peripheral area is at a distance of 3 cm, as seen in Figure 4(a). In a field area of 10×10 cm^2, the peripheral area is estimated to be at a distance of 6 cm because, as shown in Figure 4(b), at a distance of 5 cm from the center of the target volume is the OAR area. In GTV tumors with the highest intensity, the GTV is a good imaging to describe the tumor [36]. The intensity of tumor cells in the CTV is lower than in the GTV.

3.2. Peripheral dose Calculation Based on Field Edge Distance

The results of the peripheral dose calculation based on the field edge distance using the TPS calculation can be presented in Figure 5. On a field area of 5×5 cm^2, a distance of 3 cm outside the irradiation field, the dose percentage is 5–19%; at a distance of 5 cm from the edge of the field, the measured dose will decrease sharply and be below 5%, which is 1.0–3.2%. At a distance of 7 cm, the measured dose percentage is 0.6–1.7%, and at 10 cm, the dose percentage is 0.2–0.7%.

The TPS calculation results for a field area of 10×10 cm^2 at a distance of 3 cm have a high dose percentage of 99-100%; moreover, at a distance of 5 cm, the dose percentage decreases to 60–90%. At a distance of 7 cm, the dose percentage only decreases to below 10% by 2.9–7.8%, and at a distance of 10 cm from the edge of the field, the dose percentage obtained is 1.5-3.4%. At a distance of 15 cm for both the field area of 5×5 and 10×10 cm^2, the peripheral dose percentage is 0%.

Based on Figure 5, the peripheral dose decreases as the measurement distance from the edge of the radiation field increases. This trend is caused by photons follow the inverse square law, where the intensity of photon radiation will decrease in proportion to the square of the distance from the source of the initial intensity. The energy distribution factor in photons can also cause the measured dose to be smaller if the distance from the source is increased [37][38]. When the distance from the source increases, the radiation energy must be divided into a larger area. As a result, the energy per unit area decreases [39]-[41]. At a distance of 15 cm from the edge of the radiation field, the dose calculated by the TPS is 0% because, in the TPS algorithm, at 15 cm, it is considered outside the body or the PTV and OAR areas. Figure 5 also shows that the peripheral dose value for a field area of 5×5 cm^2 is smaller than that for a field area of 10×10 cm^2.

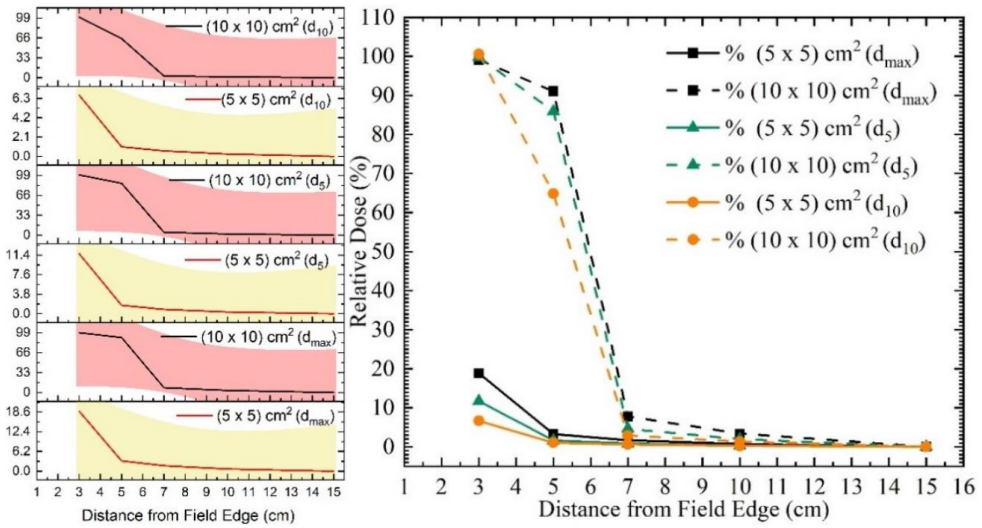

Figure 5. Peripheral dose percentage based on field edge distance.

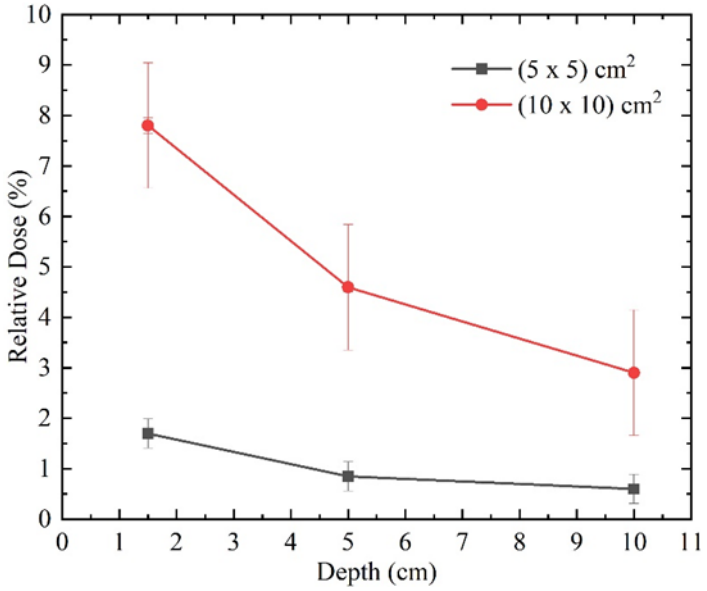

Figure 6. Peripheral dose percentage based on depth.

3.3. Peripheral dose Calculation Based on Depth

The results of peripheral dose measurements based on depth with TPS calculations can be presented in Figure 6. It can be seen in Figure 6 that at the maximum depth or depth of 1.5 cm, the dose percentage has the highest value, which is 1.70% for the field area of 5×5 cm^2 and 7.80% for the depth 10×10 cm^2. After passing the maximum depth, the dose percentage will decrease; at a depth of 5 cm, the measured dose percentage is 0.85% for the field area of 5×5 cm^2 and 4.60% for the depth of 10×10 cm^2. At a depth of 10 cm, the dose percentage decreases until it reaches 0.60% for the field area of 5×5 cm^2 and 2.90% for the depth of 10×10 cm^2.

The results of the TPS calculation show that the peripheral dose will decrease with increasing depth. When photons pass through a medium such as water, air, or other materials, the medium will absorb some of the photons. This factor is known as absorption, where the energy of the absorbed photons will be converted into the internal energy of the medium. One of the factors that affects the size of this absorption is the value of the absorption coefficient, which is influenced by the type and energy of the photons used. The higher the absorption coefficient value, the faster the decrease in radiation intensity with depth. When interacting with particles in the medium, the spread of photon radiation will also affect the value of radiation intensity with depth. This spread causes the photons to change direction; in some cases, the photons can also change energy [42]-[44].

4. CONCLUSIONS

The location of the tumor can influence the peripheral dose value. The peripheral dose in the GTV area is higher than in the CTV one. When measured relative to the distance from the field edge, the peripheral dose decreases as the measurement point moves farther away. Similarly, measurements based on depth show that the peripheral dose decreases with increasing depth. This finding is attributed to the reduction in radiation intensity due to scattering and absorption in the tissue. However, these effects vary depending on the type of radiation, the characteristics of the radiation system, and scattering factors.

AUTHOR INFORMATION

Corresponding Author

Ramacos Fardela — Department of Physics, Universitas Andalas, Padang-25175 (Indonesia);
orcid.org/0000-0002-6991-4156
Email: ramacosfardela@sci.unand.ac.id

Authors

Ega Septryan Candra — Department of Physics, Universitas Andalas, Padang-25175 (Indonesia);

orcid.org/0009-0005-3606-2072
Dian Milvita — Department of Physics, Universitas Andalas, Padang-25175 (Indonesia);
orcid.org/0009-0008-1046-1990
Dedi Mardiansyah — Department of Physics, Universitas Andalas, Padang-25175 (Indonesia);
orcid.org/0000-0001-7421-9791
Ridwan Ridwan — Siemens Healthineers Company, Forchheim-91301 (Germany);
orcid.org/0009-0007-4303-9270
Fiqi Diyona — Medical Physics, Rumah Sakit Universitas Andalas, Padang-25175 (Indonesia);
orcid.org/0000-0002-2915-7410
Almahdi Mousa — Department of Medical Radiation, University of Libya, Tripoli-13932 (Libya);
orcid.org/0000-0003-3492-3703

Author Contributions

E. S. C. and R. F. did research concept and design, data analysis and interpretation; D. M.1., A. M., and D. M.2. did article writing, and final approval of article; R. R. gave critical revision of article, data analysis and interpretation; F. D. and E. S. C. performed data collection and assembly, data analysis and interpretation.

Conflicts of Interest

The authors declare no conflict of interest.

ACKNOWLEDGEMENT

Research funded by Directorate of Research, Technology, and Community Service Directorate General of Higher Education, Research and Technology Ministry of Education, Culture, Research and Technology on Fundamental Research – Regular by research contract number: 041/E5/PG.02.00.PL/2024 Fiscal Year 2024.

REFERENCES

[1] W. D. Coolidge, L. E. Dempster, and H. E. Tanis. (1931). "High Voltage Cathode Ray and X-Ray Tubes and Their Operation". *Physics.* **1** (4): 230-244. 10.1063/1.1745004.

[2] H. Schwoerer. (2004). In: "Femtosecond Technology for Technical and Medical Applications, (Topics in Applied Physics, ch. Chapter 17". 235-254. 10.1007/978-3-540-39848-6_17.

[3] M. Cooper, P. Mijnarends, N. Shiotani, N. Sakai, and A. Bansil. (2004). X-Ray Compton Scattering. 10.1093/acprof:oso/9780198501688.001.0001.

[4] E. Rosenblatt, E. Zubizarreta, R. Camacho, and B. Vikram. (2017). In: "Radiotherapy in cancer care: facing the global challenge". International Atomic Energy Agency.

[5] I. El Naqa, R. Li, and M. J. Murphy. (2015). Machine Learning in Radiation Oncology. 10.1007/978-3-319-18305-3.

[6] E. H. Zubizarreta, E. Fidarova, B. Healy, and E. Rosenblatt. (2015). "Need for radiotherapy in low and middle income countries - the silent crisis continues". *Clinical Oncology journal.* **27** (2): 107-14. 10.1016/j.clon.2014.10.006.

[7] R. J. Fry. (2001). "Deterministic effects". *Health Physics.* **80** (4): 338-43. 10.1097/00004032-200104000-00009.

[8] T. M. Fliedner, D. H. Graessle, V. Meineke, and L. E. Feinendegen. (2012). "Hemopoietic response to low dose-rates of ionizing radiation shows stem cell tolerance and adaptation". *Dose Response.* **10** (4): 644-63. 10.2203/dose-response.12-014.Feinendegen.

[9] P. P. Connell and S. Hellman. (2009). "Advances in radiotherapy and implications for the next century: a historical perspective". *Cancer Research.* **69** (2): 383-92. 10.1158/0008-5472.CAN-07-6871.

[10] A. Marin, M. Martin, O. Linan, F. Alvarenga, M. Lopez, L. Fernandez, D. Buchser, and L. Cerezo. (2015). "Bystander effects and radiotherapy". *Reports of Practical Oncology and Radiotherapy.* **20** (1): 12-21. 10.1016/j.rpor.2014.08.004.

[11] L. E. Feinendegen, M. Pollycove, and C. A. Sondhaus. (2004). "Responses to low doses of ionizing radiation in biological systems". *Nonlinearity in Biology, Toxicology, and Medicine.* **2** (3): 143-71. 10.1080/15401420490507431.

[12] S. S. Wallace. (2002). "Biological consequences of free radical-damaged DNA bases". *Free Radical Biology and Medicine.*

33 (1): 1-14. 10.1016/s0891-5849(02)00827-4.

[13] K. R. Brown and E. Rzucidlo. (2011). "Acute and chronic radiation injury". *Journal of Vascular Surgery.* **53** (1 Suppl): 15S-21S. 10.1016/j.jvs.2010.06.175.

[14] Y. Kagan, A. M. Afanas'ev, and V. G. Kohn. (1979). "On excitation of isomeric nuclear states in a crystal by synchrotron radiation". *Journal of Physics C: Solid State Physics.* **12** (3): 615-631. 10.1088/0022-3719/12/3/027.

[15] S. Choudhary. (2018). "Deterministic and Stochastic Effects of Radiation". *Cancer therapy & Oncology International Journal.* **12** (2). 10.19080/ctoij.2018.12.555834.

[16] M. B. Sharpe. (2006). "IAEA Technical Reports Series No. 430: Commissioning And Quality Assurance Of Computerized Planning Systems For Radiation Treatment Of Cancer". *Medical Physics.* **33** (2): 561-561. 10.1118/1.2167371.

[17] R. Shende, S. J. Dhoble, and G. Gupta. (2023). "Dosimetric Evaluation of Radiation Treatment Planning for Simultaneous Integrated Boost Technique Using Monte Carlo Simulation". *Journal of Medical Physics.* **48** (3): 298-306. 10.4103/jmp.jmp_4_23.

[18] Q. Liu, J. Liang, D. Zhou, D. J. Krauss, P. Y. Chen, and D. Yan. (2018). "Dosimetric Evaluation of Incorporating Patient Geometric Variations Into Adaptive Plan Optimization Through Probabilistic Treatment Planning in Head and Neck Cancers". *International Journal of Radiation Oncology, Biology, Physics.* **101** (4): 985-997. 10.1016/j.ijrobp.2018.03.062.

[19] N. Benzazon, A. Carre, F. de Kermenguy, S. Niyoteka, P. Maury, J. Colnot, M. M'Hamdi, M. E. Aichi, C. Veres, R. Allodji, F. de Vathaire, D. Sarrut, N. Journy, C. Alapetite, V. Gregoire, E. Deutsch, I. Diallo, and C. Robert. (2024). "Deep-Learning for Rapid Estimation of the Out-of-Field Dose in External Beam Photon Radiation Therapy - A Proof of Concept". *International Journal of Radiation Oncology, Biology, Physics.* **120** (1): 253-264. 10.1016/j.ijrobp.2024.03.007.

[20] S. F. Kry, O. N. Vassiliev, and R. Mohan. (2010). "Out-of-field photon dose following removal of the flattening filter from a medical accelerator". *Physics in Medicine & Biology.* **55** (8): 2155-66. 10.1088/0031-9155/55/8/003.

[21] S. F. Kry, U. Titt, F. Ponisch, D. Followill, O. N. Vassiliev, R. A. White, R. Mohan, and M. Salehpour. (2006). "A Monte Carlo model for calculating out-of-field dose from a varian 6 MV beam". *Medical Physics.* **33** (11): 4405-13. 10.1118/1.2360013.

[22] N. Matuszak, M. Kruszyna-Mochalska, A. Skrobala, A. Ryczkowski, P. Romanski, I. Piotrowski, K. Kulcenty, W. M. Suchorska, and J. Malicki. (2022). "Nontarget and Out-of-Field Doses from Electron Beam Radiotherapy". *Life (Basel).* **12** (6). 10.3390/life12060858.

[23] J. Ng and T. Dai. (2016). "Radiation therapy and the abscopal effect: a concept comes of age". *Annals of Translational Medicine.* **4** (6): 118. 10.21037/atm.2016.01.32.

[24] G. K. Azad and C. Corner. (2015). In: "Plastic and Reconstructive Surgery". 144-152. 10.1002/9781118655412.ch13.

[25] S. Soleymanifard, S. A. Aledavood, A. V. Noghreiyan, M. Ghorbani, F. Jamali, and D. Davenport. (2016). "In vivo skin dose measurement in breast conformal radiotherapy". *Contemporary Oncology.* **20** (2): 137-40. 10.5114/wo.2015.54396.

[26] N. N. Lethukuthula, R. J. Nicolas, N. C. Lutendo, and M. Nyathi. (2024). "A Study of the TPS Based Beam-Matching Concept for Medical Linear Accelerators at a Tertiary Hospital". *International Journal of Medical Physics, Clinical Engineering and Radiation Oncology.* **13** (01): 16-25. 10.4236/ijmpcero.2024.131002.

[27] G. Martin-Martin, S. Walter, and E. Guibelalde. (2021). "Dose accuracy improvement on head and neck VMAT treatments by using the Acuros algorithm and accurate FFF beam calibration". *Reports of Practical Oncology and Radiotherapy.* **26** (1): 73-85. 10.5603/RPOR.a2021.0014.

[28] P. Urso, R. Lorusso, L. Marzoli, D. Corletto, P. Imperiale, A. Pepe, and L. Bianchi.

(2018). "Practical application of Octavius ((R)) -4D: Characteristics and criticalities for IMRT and VMAT verification". *Journal of Applied Clinical Medical Physics.* **19** (5): 517 -524. 10.1002/acm2.12412.

[29] B. E. Nelms and J. A. Simon. (2007). "A survey on planar IMRT QA analysis". *Journal of Applied Clinical Medical Physics.* **8** (3): 76-90. 10.1120/jacmp.v8i3.2448.

[30] M. W. Geurts, D. J. Jacqmin, L. E. Jones, S. F. Kry, D. N. Mihailidis, J. D. Ohrt, T. Ritter, J. B. Smilowitz, and N. E. Wingreen. (2022). "AAPM Medical Physics Practice Guideline 5.b: Commissioning and QA of treatment planning dose calculations-Megavoltage photon and electron beams". *Journal of Applied Clinical Medical Physics.* **23** (9): e13641. 10.1002/acm2.13641.

[31] P. Francescon, C. Cavedon, S. Reccanello, and S. Cora. (2000). "Photon dose calculation of a three-dimensional treatment planning system compared to the Monte Carlo code BEAM". *Medical Physics.* **27** (7): 1579-87. 10.1118/1.599024.

[32] T. Kataria, H. B. Govardhan, D. Gupta, U. Mohanraj, S. S. Bisht, R. Sambasivaselli, S. Goyal, A. Abhishek, A. Srivatsava, L. Pushpan, V. Kumar, and S. Vikraman. (2014). "Dosimetric comparison between Volumetric Modulated Arc Therapy (VMAT) vs Intensity Modulated Radiation Therapy (IMRT) for radiotherapy of mid esophageal carcinoma". *Journal of Cancer Research and Therapeutics.* **10** (4): 871-7. 10.4103/0973-1482.138217.

[33] B. Sanchez-Nieto, K. N. Medina-Ascanio, J. L. Rodriguez-Mongua, E. Doerner, and I. Espinoza. (2020). "Study of out-of-field dose in photon radiotherapy: A commercial treatment planning system versus measurements and Monte Carlo simulations". *Medical Physics.* **47** (9): 4616-4625. 10.1002/mp.14356.

[34] V. Vlachopoulou, G. Malatara, H. Delis, K. Theodorou, D. Kardamakis, and G. Panayiotakis. (2010). "Peripheral dose measurement in high-energy photon radiotherapy with the implementation of MOSFET". *World Journal of Radiology.* **2** (11): 434-9. 10.4329/wjr.v2.i11.434.

[35] S. Dieterich, C. Cavedon, C. F. Chuang, A. B. Cohen, J. A. Garrett, C. L. Lee, J. R. Lowenstein, M. F. d'Souza, D. D. Taylor, Jr., X. Wu, and C. Yu. (2011). "Report of AAPM TG 135: quality assurance for robotic radiosurgery". *Medical Physics.* **38** (6): 2914-36. 10.1118/1.3579139.

[36] J. Van de Steene, N. Linthout, J. de Mey, V. Vinh-Hung, C. Claassens, M. Noppen, A. Bel, and G. Storme. (2002). "Definition of gross tumor volume in lung cancer: inter-observer variability". *Radiotherapy and Oncology.* **62** (1): 37-49. 10.1016/s0167-8140(01)00453-4.

[37] O. V. Gul. (2024). "Experimental evaluation of out-of-field dose for different high-energy electron beams and applicators used in external beam radiotherapy". *Radiation Physics and Chemistry.* **215**. 10.1016/j.radphyschem.2023.111345.

[38] C. Oancea, C. Granja, L. Marek, J. Jakubek, J. Solc, E. Bodenstein, S. Gantz, J. Pawelke, and J. Pivec. (2023). "Out-of-field measurements and simulations of a proton pencil beam in a wide range of dose rates using a Timepix3 detector: Dose rate, flux and LET". *Physica Medica.* **106** : 102529. 10.1016/j.ejmp.2023.102529.

[39] A. M. Abdelaal, E. M. Attalla, and W. M. Elshemey. (2020). "Estimation of Out-of-Field Dose Variation using Markus Ionization Chamber Detector". *SciMedicine Journal.* **2** (1): 8-15. 10.28991/SciMedJ-2020-0201-2.

[40] R. M. Howell, S. B. Scarboro, S. F. Kry, and D. Z. Yaldo. (2010). "Accuracy of out-of-field dose calculations by a commercial treatment planning system". *Physics in Medicine & Biology.* **55** (23): 6999-7008. 10.1088/0031-9155/55/23/S03.

[41] F. Faghihi Moghaddam, M. Bakhshandeh, M. Ghorbani, and B. Mofid. (2020). "Assessing the out-of-field dose calculation accuracy by eclipse treatment planning system in sliding window IMRT of prostate cancer patients". *Computers in Biology and Medicine.* **127** :

104052. 10.1016/j.compbiomed.2020.104052.

[42] E. M. Attalla, D. M. Sinousy, H. F. Ibrahim, F. A. Elhussiny, and A. F. Elmekawy. (2023). "The accuracy of out of field dose calculations in commercial treatment planning system using GATE/GEANT4 Monte Carlo simulation". *Radiation Physics and Chemistry.* **206**. 10.1016/j.radphyschem.2023.110772.

[43] M. Mazonakis and J. Damilakis. (2021). "Out-of-field organ doses and associated risk of cancer development following radiation therapy with photons". *Physica Medica.* **90** : 73-82. 10.1016/j.ejmp.2021.09.005.

[44] N. S. Momeni, S. Afraydoon, N. Hamzian, A. Nikfarjam, M. Vakili Ghasemabad, S. Abdollahi-Dehkordi, M. Shabani, M. Dehestani, and A. Heidari. (2023). "The Estimation of Radiation Dose to Out-of-Field Points of Organs at Risk in Block and MLC Shielded Fields in Lung Cancer Radiation Therapy". *Frontiers in Biomedical Technologies.* 10.18502/fbt.v10i2.12223.